One-way operators in laterally varying media

*C.P.A. Wapenaar, * J.L. T Grimbergen, and Frank J. Dessing, Delft University of Technology*

Summary

The usual assumption in one-way propagation is that the propagation velocity may be kept constant within the lateral support of the operator. For rapidly varying medium parameters this approach leads to inaccurate and sometimes even unstable results. In this paper we propose one-way operators (based on modal decomposition) that properly account for the lateral variations of the medium parameters and that are unconditionally stable. We illustrate with some examples that these operators are accurate for all propagation angles between -90 and +90 degrees.

Introduction

In the past twelve years much research has been done on the optimization of one-way operators for recursive wave field extrapolation. For 2-D extrapolation we mention Berkhout (1982), van der Schoot et al. (1984) and Holberg (1988); for 3-D extrapolation some representative references are Blacquiere et al. (1989) and Hale (1991). Thorbecke and Berkhout (1994) give an extensive overview. In all the references mentioned above it is assumed that the medium parameters are constant within the support of the operator. Lateral variations are taken into account by selecting for each gridpoint an operator related to the *local* medium parameters (generally only the propagation velocity) at that gridpoint. In this paper we will call this the "standard method". When the medium parameters vary smoothly (in comparison with the wavelength), this standard method yields reasonably accurate results. When the parameters vary significantly within the support of the operator, the standard method becomes inaccurate. For very rapid variations (in comparison with the wavelength) the standard method may become unstable, even when the used operators would give stable results in a homogeneous medium (Etgen, 1994). In this paper we show how to account properly for the lateral variations of the medium parameters in one-way wave field extrapolation. Essentially this comes to solving the (flux normalized) one-way *primary* propagator $W_p^{\pm}$ from the one-way wave equation

$$\frac{\partial W_p^{\pm}}{\partial z} = \mp j \hat{H}_1 W_p^{\pm}, \tag{1}$$

where the *square-root operator* $\hat{H}_1$ is implicitly defined by

$$\hat{H}_1 \hat{H}_1 = \hat{H}_2 = \frac{W^2}{c^2} + \frac{\partial^2}{\partial x^2}. \tag{2}$$

(Throughout this paper the hats (^) denote *operators* containing the lateral differentiation operator $\partial/\partial x$; for convenience we consider the 2-D situation). This approach is strictly valid only for media in which the density is constant. For the extension to variable density media, see our DELPHI consortium publications.
In this paper we apply modal decomposition to the operator $\hat{H}_2$ for laterally varying media and we derive, subsequently, the square-root operator $\hat{H}_1$ and the primary propagator $W_p^{\pm}$. The theory is illustrated with numerical examples.

The square-root operator

The kernel of the square-root operator

By letting the operator $\hat{H}_n(x,z)$, ($n = 1,2$) act on an arbitrary test function $F(x,z)$ (with "sufficient decay" at infinity), we introduce its kernel $H_n(x, z; x')$, according to

$$\hat{H}_n(x,z)F(x,z) = \int_{-\infty}^{\infty} H_n(x,z;\, x')F(x',z)dx'. \tag{3}$$

For $n = 2$ we have

$$H_2(x,z;\, x') = \left(\frac{\omega}{c(x,z)}\right)^2 \delta(x-x') + d_2(x-x'), \tag{4}$$

where

$$d_2(x-x') = \frac{\partial^2 \delta(x-x')}{\partial x^2}. \tag{5}$$

This result is easily verified by substitution in equation (3) and using the sift property of the delta function. For a further discussion of the delta function and its derivatives, see Bleistein (1984). Note that $H_2(x, z; x')$ is symmetric and real-valued, according to

$$H_2(x,z;x') = H_2(x',z;x) = H_2^*(x',z;x), \tag{6}$$

where * denotes complex conjugation. In analogy with equation (2), the kernels of $\hat{H}_2$ and $\hat{H}_1$ are related, according to

$$H_2(x,z;x') = \int_{-\infty}^{\infty} H_1(x,z;x'')H_1(x'',z;x')dx''. \tag{7}$$

Hence, resolving the square-root operator $\hat{H}_1(x,z)$ from equation (2) is equivalent to resolving the kernel $H_1(x, z; x'')$ from equation (7). This is extensively discussed by Grimbergen (1995). Here we proceed directly with a numerical procedure. To this end we first briefly review Berkhout's matrix notation.

The square-root operator in matrix form

We introduce a *matrix* $\mathbf{H}_n(z)$ that contains the discretized version of the kernel $H_n(x,z;x')$ at depth level z, according to

$$\mathbf{H}_n(z) = \Delta x \begin{pmatrix} H_n(x_1,z;\,x_1) & \cdots & H_n(x_1,z;\,x_M) \\ \vdots & \ddots & \vdots \\ H_n(x_M,z;\,x_1) & \cdots & H_n(x_M,z;\,x_M) \end{pmatrix}, \tag{8}$$

where Ax is the horizontal discretization interval. In particular, for $n = 2$ we obtain from equations (4) and (8)

$$\mathbf{H}_2(z) = \mathbf{C}(z) + \mathbf{D}_2, \tag{9}$$

where $\mathbf{C}(z)$ is a diagonal matrix containing the discretized version of $\{\omega/c(x,z)\}^2$ at depth level z, according to

$$\underset{\sim}{C}(z) = \begin{pmatrix} \left(\frac{\omega}{c(x_1,z)}\right)^2 & 0 & \cdots & 0 \\ 0 & \left(\frac{\omega}{c(x_2,z)}\right)^2 & \cdots & 0 \\ \vdots & \vdots & \ddots & \vdots \\ 0 & 0 & \cdots & \left(\frac{\omega}{c(x_M,z)}\right)^2 \end{pmatrix} \quad (10)$$

and where $\underset{\sim}{D}_2$ contains the discretized version of the second order differentiation filter $d_2(x)$. For "sufficiently small" Δx this matrix may be written as

$$\underset{\sim}{D}_2 = \frac{1}{\Delta x^2} \begin{pmatrix} -2 & 1 & 0 & \cdots & 0 & 0 & 0 \\ 1 & -2 & 1 & \cdots & 0 & 0 & 0 \\ \vdots & \vdots & \vdots & \ddots & \vdots & \vdots & \vdots \\ 0 & 0 & 0 & \cdots & 1 & -2 & 1 \\ 0 & 0 & 0 & \cdots & 0 & 1 & -2 \end{pmatrix}. \quad (11)$$

However, in practice we use a higher order approximation. In this matrix notation, the symmetry property (6) reads

$$\underset{\sim}{H}_2(z) = \underset{\sim}{H}_2^T(z) = \underset{\sim}{H}_2^H(z), \quad (12)$$

where ^{T} denotes transposition and where ^{H} denotes transposition and complex conjugation. Finally, equation (7) reads in the matrix notation

$$\underset{\sim}{H}_2(z) = \underset{\sim}{H}_1(z)\underset{\sim}{H}_1(z). \quad (13)$$

Hence, resolving the square-root operator $H_1(x, z)$ from equation (2), or resolving the kernel $H_1(x, z; x'')$ from equation (7), is equivalent to resolving the matrix $\underset{\sim}{H}_1$ (x) from equation (13).

Determining the square-root operator

As we will see below, modal decomposition can be accomplished by applying eigenvalue decomposition to the matrix $\underset{\sim}{H}_2(z)$:

$$\underset{\sim}{H}_2(z) = \underset{\sim}{L}(z)\underset{\sim}{\Lambda}(z)\underset{\sim}{L}^{-1}(z), \quad (14)$$

where

$$\underset{\sim}{\Lambda}(z) = \mathrm{diag}\Big(\lambda_1(z) \cdots \lambda_m(z) \cdots \lambda_M(z)\Big). \quad (15)$$

The eigenvalues X,(x) are real valued as a result of symmetry property (12). Using a proper scaling of the eigenvectors, $\underset{\sim}{L}^{-1}(z)$ is related to $\underset{\sim}{L}(z)$, according to

$$\underset{\sim}{L}^{-1}(z) = \underset{\sim}{L}^H(z). \quad (16)$$

Now for $\underset{\sim}{H}_1(z)$ we may write

$$\underset{\sim}{H}_1(z) = \underset{\sim}{L}(z)\underset{\sim}{\Lambda}^{1/2}(z)\underset{\sim}{L}^H(z \;, \quad (17$$

which is easily verified by substitution in equation (13) and comparing the result with equation (14). From equation (15) we obtain

$$\underset{\sim}{\Lambda}^{1/2}(z) = \mathrm{diag}\Big(\lambda_1^{1/2}(z) \cdots \lambda_m^{1/2}(z) \cdots \lambda_M^{1/2}(z)\Big). \quad (18)$$

The sign of $\lambda_m^{1/2}$(z) is chosen such that when X,(x) is positive, then

$$\Re\{\lambda_m^{1/2}(z)\} \geq 0, \quad (19)$$

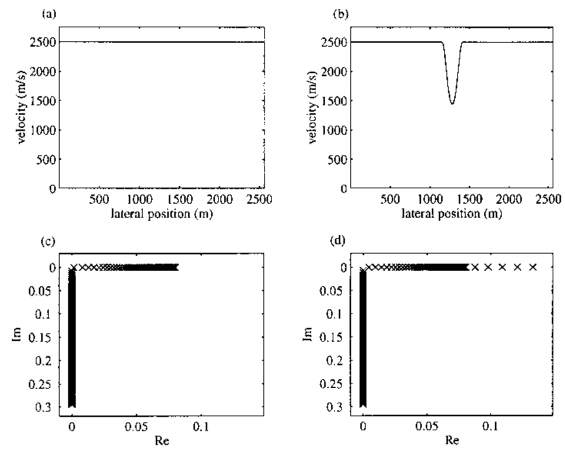

Figure 1: *The location of the eigenvalues $\lambda_m^{1/2}$ of the square-root operator in the complex plane. (a) Homogeneous medium. (b) Laterally variant medium. (c) Eigenvalues for homogeneous medium. (d) Eigenvalues for laterally variant medium.*

and when X,(x> is negative, then

$$\Im\{\lambda_m^{1/2}(z)\} \leq 0. \quad (20)$$

In Figure 1 we have, for two media, depicted the location of the eigenvalues $\lambda_m^{1/2}$ of $\underset{\sim}{H}_1$ in the complex plane. For both examples in this section, the temporal frequency ω=200 rad/s and the spatial sampling interval Δx=10 m.

In the homogeneous case (Figures 1a,c), the eigenvalues of $\underset{\sim}{H}_1$ are densely distributed along parts of the real and imaginary axes. In principle, any point in between the indicated eigenvalues belongs to the admissible values of $\lambda^{1/2}$. Because of the finite extent of the matrix $\underset{\sim}{H}_2$, the "branches" on the axes are not continuous. The maximum eigenvalue on the real axis corresponds to $\lambda^{1/2}$ = w/c = 0.08, which represents a plane wave (or *eigenmode),* propagating vertically downwards. The other eigenvalues on the real axis correspond to obliquely propagating plane waves (eigenmodes), with vertical phase velocity $c_{z,m} = \omega\lambda_m^{-1/2}$. The eigenvalues on the imaginary axis correspond to evanescent waves. The minimum eigenvalue on the imaginary axis has no physical meaning. It is the result of the discretization of the matrix $\underset{\sim}{H}_2$.

For laterally varying media (Figures 1b,d), the eigenvalues on the real axis correspond to propagating eigenmodes, the vertical phase velocity again being given by $c_{z,m} = \omega\lambda_m^{-1/2}$. An interesting situation occurs here, since the medium shows locally a velocity-dip. Eigenvalues up to $\lambda^{1/2} = \omega/c_{min}$, where c_{min} is the minimum velocity in the medium, become admissible. The corresponding eigenmodes are vanishing outside this low-velocity region and are therefore "trapped" in the disturbance. We call these *guided modes.* Figure 1d shows that for this medium configurat ion, the eigenvalue-spect rum contains, besides the "continuous" branches, a finite number of discrete eigenvalues which belong to these guided modes.

For the homogeneous as well as for the laterally variant situation, the eigenmodes are contained in the columns of the matrix $\underset{\sim}{L}$. Figure 2 shows the structure of all the matrices involved in equation (17).

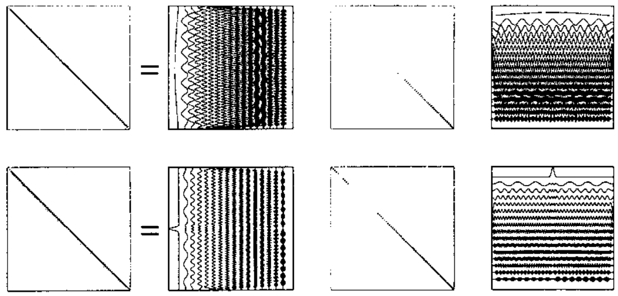

Figure 2: Schematical representation of the eigenvalue decomposition of the square-root operator for the homogeneous situation (top) and for the laterally variant situation [bottom).

The primary propagator

Kernel and matrix form

The primary propagator $W_p^{\pm}$ satisfies the following equation (conform equation 1)

$$\frac{\partial W_p^{\pm}(x,z;x',z')}{\partial z} = \mp j \hat{H}_1(x,z) W_p^{\pm}(x,z;x',z'), \tag{21}$$

where $W_p^{\pm}(x, z=z'; x', z') = \delta(x-x')$. Replacing the operator $\hat{H}_1$ by its kernel, yields

$$\frac{\partial W_p^{\pm}(x,z;x',z')}{\partial z} = \mp j \int_{-\infty}^{\infty} H_1(x,z;x'') W_p^{\pm}(x'',z;x',z') dx''. \tag{22}$$

We define a *matrix* $\mathbf{W}_p^{\pm}(z,z')$ that contains the discretized version of the propagator $W_p^{\pm}(x,z;x',z')$, according to

$$\mathbf{W}_p^{\pm}(z,z') = \Delta x \begin{pmatrix} W_p^{\pm}(x_1,z;\ x_1,z') & \cdots & W_p^{\pm}(x_1,z;x_M,z') \\ \vdots & \ddots & \vdots \\ W_p^{\pm}(x_M,z;x_1,z') & \cdots & W_p^{\pm}(x_M,z;x_M,z') \end{pmatrix}$$

In this matrix notation, equation (22) transforms to

$$\frac{\partial \mathbf{W}_p^{\pm}(z,z')}{\partial z} = \mp j\, \mathbf{H}_1(z) \mathbf{W}_p^{\pm}(z,z'), \tag{23}$$

where $\mathbf{W}_p^{\pm}(z=z',z') = \mathbf{I}$. Hence, resolving the primary propagator $W_p^{\pm}(x,z;x',z')$ from equation (21) is equivalent to resolving the matrix $\mathbf{W}_p^{\pm}(z,z')$ from equation (23).

Determining the primary propagator

From here onwards we will assume for convenience that the medium parameters do not vary in the depth direction between z' and z. This is a reasonable assumption when $|z-z'|$ is "sufficiently small". (For the more general situation, see Wapenaar and Berkhout, 1989, Chapter 3). Using a Taylor series expansion, we may write

$$\mathbf{W}_p^{\pm}(z,z') = \sum_{k=0}^{\infty} \frac{(z-z')^k}{k!} (\mp j)^k \mathbf{H}_1^k(z'), \tag{24}$$

or, symbolically,

$$\mathbf{W}_p^{\pm}(z,z') = \exp\{\mp j(z-z')\mathbf{H}_1(z')\}. \tag{25}$$

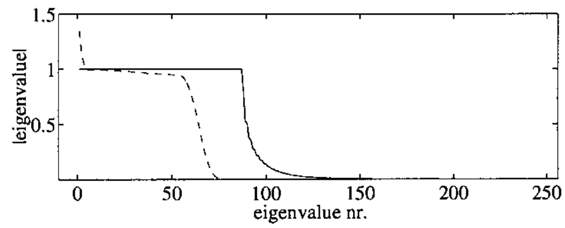

Figure 3: Absolute value of the eigenvalues (in descending order) of the primary propagator, calculated by modal decomposition (solid) and by the "standard method" (dashed). The extrapolation distance $|z-z'| = 50m$.

From equations (16) and (17), we obtain

$$\mathbf{H}_1^k(z') = \mathbf{L}(z')\mathbf{\Lambda}^{k/2}(z')\mathbf{L}^{-1}(z'). \tag{26}$$

Substitution in equation (24) gives

$$\mathbf{W}_p^{\pm}(z,z') = \mathbf{L}(z')\left[\sum_{k=0}^{\infty} \frac{(z-z')^k}{k!}(\mp j)^k \mathbf{\Lambda}^{k/2}(z')\right] \mathbf{L}^{-1}(z'), \tag{27}$$

or, using (16)

$$\mathbf{W}_p^{\pm}(z,z') = \mathbf{L}(z')\breve{\mathbf{W}}_p^{\pm}(z,z')\mathbf{L}^H(z'), \tag{28}$$

where, symbolically,

$$\breve{\mathbf{W}}_p^{\pm}(z,z') = \exp\{\mp j(z-z')\mathbf{\Lambda}^{1/2}(z')\}. \tag{29}$$

Using equation (18) we obtain

$$\breve{\mathbf{W}}_p^{\pm}(z,z') = \begin{pmatrix} \exp\{\mp j(z-z')\lambda_1^{1/2}(z')\} & \cdots & 0 \\ \vdots & \ddots & \vdots \\ 0 & \cdots & \exp\{\mp j(z-z')\lambda_M^{1/2}(z')\} \end{pmatrix}. \tag{30}$$

From equations (19), (20) and (30) we find that the eigenvalues of $\mathbf{W}_p^{\pm}(z,z')$ all have absolute values smaller than or equal to unity. This property guarantees the stability of this propagator when applied recursively, because no wave mode can erroneously be amplified. For the laterally variant medium of Figure lb we have depicted in Figure 3 the eigenvalues of the primary propagator $\mathbf{W}_p^{\pm}(z,z')$. For comparison, the eigenvalues of the propagator matrix obtained according to the "standard method" (see the introduction) are also shown (dashed). It is clear from this figure that for the standard method there are certain eigenvalues having absolute values considerably larger than unity. It turns out that the corresponding eigenmodes are guided eigenmodes. We may expect that in recursive applications these eigenmodes are erroneously amplified, as was demonstrated by Etgen (1994). Finally, note that (also for the standard method) the eigenvalues beyond nr. 60 decay rapidly, meaning that (in this specific example) propagation angles beyond 50 degrees are erroneously suppressed.

Numerical examples of the primary propagator

The performance of the proposed primary propagator is now compared to the standard method and to finite difference modeling.

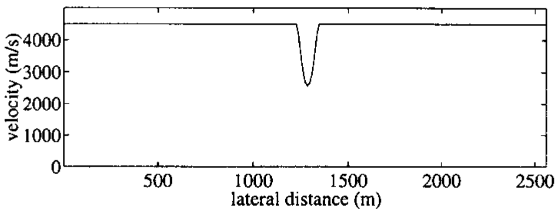

Figure 4: *Medium in which modeling takes place. The lateral extent of the disturbance is approximately equal to the wavelength.*

For this purpose we consider a medium in which the velocity depends only on the lateral coordinate x (Figure 4). The lateral extent of the disturbance in the medium is approximately equal to the central wavelength of the modeled wave field. The source function contains frequencies up to 60Hz. For the spatial sampling interval again Δx=10m is taken. Finite difference modeling needed a three times finer sampling for the stability criteria to be met. At a specific depth level a vertically downward propagating plane wave is excited. Recording takes place at a 1000m lower depth level. The results are shown in Figure 5. It is clear that the standard method (Figure 5b) suffers from the erroneous amplification of the wave field in the low-velocity region. The strong anticausal effects are the result of time wrap-around. The modal decomposition (Figure 5c) produces plane wave responses in accordance with finite difference modeling (apart from some finite aperture artefacts). The result remains fully stable and shows excellent handling of high angle wave field constituents. Of course one must be cautious using the results of finite difference modeling as a reference. The large velocity disturbance is sampled with a relatively small number of samples which can cause finite difference results to become unreliable.

Conclusions

Modal decomposition of acoustic wave fields is a method that accounts correctly for lateral gradients in one-way operators, for example in the square-root operator $\underset{\sim}{\mathbf{H}}_1$ (z) and in the primary propagator $\underset{\sim}{\mathbf{W}}_p^{\pm}(z,z')$. Mat hematically, the modal decomposition of the wave field is equivalent to the eigenvalue decomposition of $\underset{\sim}{\mathbf{H}}_2(z)$. The eigenvectors physically represent wave constituents having a vertical phase velocity $c_{z,m} = \omega\lambda_m^{-1/2}$, where λ_m is the corresponding eigenvalue.

The application of this method currently requires more computation time than the "standard method". However, when lateral variations cannot be ignored on a wavelength scale, the "standard method" breaks down. The results become erroneous and in certain medium configurations the standard primary propagator even turns out to be unstable. In this case the modal decomposition of the wave field can become cost-effective. The results of the modal decomposition method in laterally variant media show that the operators are unconditionally stable and very accurate. In principle angles up to 90 degrees and a considerable part of the evanescent field are handled correctly.

With respect to this high performance the question arises whether we can exchange unnecessary accuracy for computational efficiency. This is the subject of current investigations in our DELPHI consortium project.

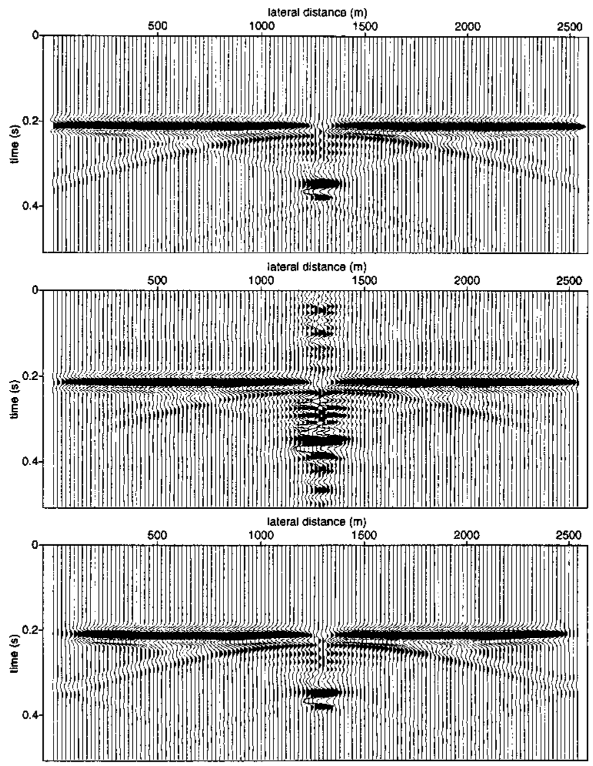

Figure 5: *Results of* 1000m *extrapolation: finite difference (top), standard method (middle) and modal decomposition (bottom).*

References

Berkhout, A. J., 1982, Seismic migration, Elsevier Science Publ.

Blacquiere, G., Debeye, H.W. J., Wapenaar, C.P.A., and Berkhout, A. J., 1989, 3-D table driven migration, Geophysical Prospecting, 37, 925-958.

Bleistein, N., 1984, Mathematical methods for wave phenomena: Academic Press,Inc., Orlando.

Etgen, J.T., 1994, Stability of explicit depth extrapolation through laterally-varying media: 64th Annual Internat. Mtg., Soc. Expl. Geophys., Expanded Abstracts, Soc. Expl. Geophys., 1266-1269.

Grimbergen, J.L.T., 1995, One-way wave field operators in laterally varying media: M. SC. thesis, Delft Univ. of Techn.

Hale, D., 1991, 3-D depth migration via McClellan transformations, Geophysics, 56, 1778-1785.

Holberg, O., 1988, Towards optimum one-way wave propagation: Geophysical Prospecting, 36, 99-114.

van der Schoot, A., Vos, H.C.L., and Berkhout, A. J., 1984, Finite-difference formulations of the wave equation in the space-frequency ($x-\omega$)-domain: 46th EAEG meeting, London, 67.

Thorbecke, J. W. and Berkhout, A. J., 1994, 3-D recursive extrapolation operators: An overview: 64th Annual Internat. Mtg., Soc. Expl. Geophys., Expanded Abstracts, Soc. Expl. Geophys., 1262-1265.

Wapenaar, C.P.A., and Berkhout, A.J., 1989, Elastic wave field extrapolation: Elsevier Science Publ.